



HAL
open science

Intensification of p-coumaric acid heterologous production using extractive biphasic fermentation

Jeanne Combes, Nabila Imatoukene, Julien Couvreur, Blandine Godon, Fanny Brunissen, Clémentine Fojcik, Florent Allais, Michel Lopez

► To cite this version:

Jeanne Combes, Nabila Imatoukene, Julien Couvreur, Blandine Godon, Fanny Brunissen, et al.. Intensification of p-coumaric acid heterologous production using extractive biphasic fermentation. *Biore-source Technology*, 2021, 337, pp.125436. 10.1016/j.biortech.2021.125436 . hal-03589796

HAL Id: hal-03589796

<https://agroparistech.hal.science/hal-03589796>

Submitted on 2 Aug 2023

HAL is a multi-disciplinary open access archive for the deposit and dissemination of scientific research documents, whether they are published or not. The documents may come from teaching and research institutions in France or abroad, or from public or private research centers.

L'archive ouverte pluridisciplinaire **HAL**, est destinée au dépôt et à la diffusion de documents scientifiques de niveau recherche, publiés ou non, émanant des établissements d'enseignement et de recherche français ou étrangers, des laboratoires publics ou privés.



Distributed under a Creative Commons Attribution - NonCommercial 4.0 International License

12 **Abstract**

13 *p*-coumaric acid (*p*-CA) can be produced from D-glucose by an engineered *S. cerevisiae*
14 strain. *p*-CA has antimicrobial properties and retro-inhibition activity. Moreover, *p*-CA
15 is a hydrophobic compound, limiting its accumulation in fermentation broth. To
16 overcome these issues all at once, a liquid-liquid extraction *in-situ* product recovery
17 process using oleyl alcohol as extractant has been implemented in order to continuously
18 extract *p*-CA from the broth. Media and pH impacts on strain metabolism were
19 assessed, highlighting *p*-CA decarboxylase endogenous activity. Biphasic fermentations
20 allowed an increase in *p*-CA respiratory production rates at both pH assessed (13.65 and
21 9.45 mg.L⁻¹.h⁻¹ at pH 6 and 4.5, respectively) compared to control ones (10.5 and 7.5
22 mg.L⁻¹.h⁻¹ at pH 6 and 4.5, respectively). Biphasic fermentation effects on *p*-CA
23 decarboxylation were studied showing that continuous removal of *p*-CA decreased its
24 decarboxylation into 4-vinylphenol at pH 4.5 (57 mg.L⁻¹ in biphasic fermentation vs 173
25 mg.L⁻¹ in control one).

26

27 **Keywords**

28 *p*-coumaric acid, *In situ* product recovery, engineered *Saccharomyces cerevisiae*, 4-
29 vinylphenol, biphasic fermentation

30 1. Introduction

31 *p*-coumaric acid (*p*-CA) is an *p*-hydroxycinnamic acid (HCA), a ubiquitous specialized
32 metabolite in plants and some fungi, and the precursor of a wide range of other valuable
33 molecules, among others: HCAs, flavonoids, and lignin (Higuchi, 1981; Humphreys
34 and Chapple, 2002). Moreover, *p*-CA has numerous applications in food, cosmetic and
35 pharmaceutical industries thanks to its numerous biological activities (e.g. antioxidant,
36 antimicrobial, anti-viral, antimutagenesis, anti-cancer activities) (Pei et al., 2016; Boo,
37 2019). Although *p*-CA can be either extracted from biomass or chemically produced
38 through a Knoevenagel-Doebner condensation, both approaches have some drawbacks
39 such as the availability of natural raw materials at low cost and large quantities, the use
40 of hazardous solvents, and the production of organic wastes (Flourat et al., 2020).
41 Aromatic amino acids (AAA) – precursors of *p*-CA in the phenylpropanoid pathway
42 (Herrmann and Weaver, 1999) – can be produced by microorganisms (e.g.
43 *Saccharomyces cerevisiae*) through the shikimate pathway (following carbohydrates
44 metabolism). Therefore, there has been a great deal of works dedicated to the
45 engineering of microorganisms to produce AAA-derived compounds (e.g. HCA) from
46 sugar such as D-glucose (Averesch and Kayser, 2020; Huccetogullari et al., 2019).
47 To produce *p*-CA heterologously from glucose using a *S. cerevisiae* strain, a lot of
48 effort has been made on rewiring carbon flux into AAA metabolism and impair retro-
49 inhibition to maximize the pool of L-tyrosine (Tyr) and L-phenylalanine (Phe),
50 precursors of *p*-CA and cinnamic acid, respectively (Hartmann et al., 2003; Q. Liu et al.,
51 2019; Luttik et al., 2008; Rodriguez et al., 2015). Moreover, Tyr/Phe ammonia lyase
52 (TAL/PAL) and a cinnamic acid-4-hydroxylase (C4H), that deaminate Tyr and Phe and
53 allows the hydroxylation of cinnamic acid to form *p*-CA, respectively, have been

54 expressed in *S. cerevisiae*. It is worth mentioning that many studies have investigated
55 new enzymes from fungi, bacteria and plants to discover those with higher or more
56 stable catalytic activity (Hyun et al., 2011; Jendresen et al., 2015; Varga et al., 2017).
57 Another common strategy to engineer *S. cerevisiae* into a *p*-CA producing host consists
58 in deleting endogenous genes encoding the major Ehrlich pathway phenylpyruvate
59 decarboxylases (Hazelwood et al., 2008; Koopman et al., 2012).
60 While progress is continuously made in the molecular biology part of *p*-CA production
61 using *S. cerevisiae*, there are still several issues to address. *p*-CA has been studied for its
62 antimicrobial properties, therefore, it can be expected that there is a limitation on *p*-CA
63 accumulation in fermentation broth due to its toxicity against the producer
64 microorganisms (Baranowski et al., 1980; Davidson et al., 2013; J. Liu et al., 2020). *p*-
65 CA precursors and *p*-CA can also be degraded by endogenous *S. cerevisiae* enzymes
66 and, although the strategy against major Ehrlich pathway decarboxylases seems to be
67 efficient, there might be still some *p*-CA or precursors co-products formed due to the
68 high number of endogenous decarboxylases in *S. cerevisiae* (Hazelwood et al., 2008;
69 Koopman et al., 2012). There is also an end-product inhibition effect on TAL/PAL by
70 *p*-CA and thus its accumulation in the broth could inhibit the productivity when it
71 reaches a certain titer (Sariaslani, 2007). Furthermore, *p*-CA being a hydrophobic
72 solute, as indicated by its predicted partition coefficient between octanol and water,
73 $\text{Log}(P_{o/w})$, of 1.59 (predicted using KOWWINTM v 1.68), its accumulation in the
74 fermentation broth is also limited by *p*-CA maximal solubility in aqueous media (0.838
75 $\pm 0.003 \text{ g.L}^{-1}$ at $30 \text{ }^\circ\text{C}$ in water) (Combes et al., 2021). For instance, Q. Liu et al. (2019)
76 reached a titer of 12.5 g.L^{-1} *p*-CA with a *S. cerevisiae* strain using fed-batch
77 fermentation process and noticed *p*-CA crystallization in the broth.

78 While this biotechnological production approach is promising and there is still room for
79 optimization for microorganisms engineering, there is a lack of research in both
80 fermentation process optimization and downstream processing of HCA. To prevent
81 product toxicity, one can use a robust host that can tolerate high concentrations of this
82 solute. For instance, Nijkamp et al. (2007) used a solvent-tolerant strain, *Pseudomonas*
83 *putida* S12 as *p*-CA producer frame (Nijkamp et al., 2007). Another strategy that can
84 meet every need and ease the downstream process consists in performing an extractive
85 fermentation by setting up an *in situ* product recovery (ISPR) process. In the case of
86 hydrophobic solute, a liquid-liquid extraction (LLE) using an organic immiscible
87 solvent coupled with the fermentation shall allow medium detoxification, prevent
88 product degradation, and overcome the solubility limit (Cuellar and Straathof, 2018).
89 ISPR process not only improves yield and productivity, but also simplifies the product
90 recovery (Freeman et al., 1993). In the last twenty years, several reviews have been
91 published on ISPR processes coupled with bioconversions including LLE-ISPR,
92 providing details on industrial applications and lab scale results for a broad range of
93 bio-products. They demonstrate the great potential of ISPR and the need of
94 straightforward processes for future industrial applications (Dafoe and Daugulis, 2014;
95 Santos et al., 2020; Van Hecke et al., 2014; Yang and Lu, 2013).
96 Herein, the first implementation and assessment of a LLE-ISPR process was described
97 for the intensification of heterologous *p*-CA production by a strain of *S. cerevisiae*
98 (referred at as ABG010) with oleyl alcohol as extractant (Combes et al. 2021). Prior to
99 performing biphasic fermentations, as medium and pH impact metabolism, growth,
100 recovery and process cost, the strain metabolism has been studied in different control
101 batches using rich and complex or chemically defined medium and pH 4.5 and 6.

102

103 2. Materials and methods

104 2.1. Chemicals

105 *cis*-9-Octadecen-1-ol (oleyl alcohol, OA) was purchased from Merck KGaA ($\geq 80\%$).

106 Standard of *trans*-*p*-coumaric acid and *trans*-ferulic acid were purchased from TCI (\geq

107 98%). Standard of 4-vinylphenol (4-*vp*) was chemically synthesized in-house and

108 characterized by ^1H NMR from *trans*-*p*-coumaric acid following an adaptation of **a**

109 previous work in 2018 (Mouterde and Allais, 2018).

110

111 2.2. ABG010: Engineered *S. cerevisiae* relevant characteristics

112 *S. cerevisiae* S288C (Mortimer and Johnston, 1986), uracil, tryptophan and leucine

113 auxotrophic was used. This yeast model strain (**ABG010**) was engineered **and provided**

114 **by Abolis (France)** to produce *p*-CA with optimized performances: **(i)** ARO10

115 (YDR380W) and Thi3(YDL080C) genes were deleted, **(ii)** ARO4 (NP_009808) and

116 ARO7 (NP_015385) were amplified by PCR from the genomic DNA of *S. cerevisiae*

117 and mutated to resist to feedback inhibition (FBR: Feed Back Resistance) (Gold et al.,

118 2015), **(iii)** TAL, PAL, C4H and Cpr1 were optimized for yeast codon usage bias then

119 synthesized by DC Biosciences, Dundee, UK. Characteristics of the final strain

120 ABG010 are: MAT α , *ura3-52*, *trp1* Δ 63, *leu2* Δ 1, GAL2+, LEU2+, *aro10* Δ 0, *thi3* Δ 0,

121 FAT3~MTR2::(*ARO4fbr*-*ARO7fbr*-RgTAL)::URA3, NCA3~ASF1::(*AtPAL*-*AtC4H*-

122 CrCPR1)::TRP1.

123

124 2.3. Media composition & fermentation conditions

125 Yeast Nitrogen Base medium without amino acids (YNB w/o aa) was purchased from
126 Sigma Aldrich. A 10X stock solution was prepared following the supplier instructions
127 using elix water and sterilized by filtration. The final medium consisted of 2X YNB w/o
128 aa with 20 g.L⁻¹ of D-glucose (from Alfa Aesar, anhydrous, 99%). Yeast extract
129 peptone dextrose medium (YEPD) consisted of 20 g.L⁻¹ of peptone (from Fisher
130 Scientific), 10 g.L⁻¹ of yeast extract (from Fisher Scientific), and 20 g.L⁻¹ of D-glucose
131 (from Alfa Aesar, anhydrous, 99%). This medium was sterilized by autoclaving at 121
132 °C for 20 min.

133 For every experiment, the strain was pre-cultured in 50 mL of YEPD in a baffled
134 Erlenmeyer overnight at 30 °C and 180 rpm from an inoculum kept at -80 °C.
135 Bioreactors were inoculated with pre-culture to reach an initial optical density at 620
136 nm (OD_{620 nm}) of 0.2. Experiments were made at least in duplicate unless otherwise
137 specified.

138 All experiments were conducted in 1.5 L bioreactors with a PRO-LAB™ controller
139 unit, C-BIO2™ operator and control software from Global Process Concept (GPC, La
140 Rochelle, France). Bioreactors were equipped with pH and dissolved oxygen (DO)
141 probes from Hamilton Company. Temperature was regulated at 30 °C, the aeration rate
142 was constant through an experiment and mixing rate was used to regulate DO levels
143 unless stated otherwise. The working pH (4.5 or 6) was maintained using KOH 1 M or
144 H₂SO₄ 0.5 M solutions.

145 For one phase batch experiments, fermentation working volume was 1 L. Air was
146 delivered through a nutsparger (GPC, La Rochelle, France) in bioreactors and the

147 airflow was maintained at 0.5 L.min⁻¹. The DO was set up at 30% saturation level and
148 was controlled by stirring at a rate between 350 and 900 rpm.

149 For biphasic aerobic bioconversions, the configuration and operating methods are
150 crucial. Indeed, if cells are mixed vigorously with the water-immiscible solvent, a stable
151 emulsion could appear due to the presence of surface-active components (Heeres et al.,
152 2014; Stark and Stockar, 2003). Cells can also promote Pickering emulsions (Heeres et
153 al., 2014). To overcome water/oil emulsion, agitation was fixed at 75 rpm and to
154 promote coalescence inside the bioreactor, 0.004% (v/v) Tween 80 was added when
155 necessary. To address the low stirring rate, sintered-microsparger (0.2 µm pores) was
156 used for a suitable aeration in those biphasic and control fermentations and an airflow of
157 0.1 L.min⁻¹. Working volume for fermentation medium was 0.5 L and the same volume
158 of OA was added at the beginning or after 24 h of cultivation.

159

160 2.4. Identification of broth phenolic compounds by liquid chromatography-mass 161 spectrometry

162 Identification of phenolic compounds was performed on an Agilent Infinity 1290
163 system, equipped with a 6545 Q-TOF mass spectrometer (Wilmington, DE, USA) and a
164 PDA UV detector using a Zorbax C18 column from Agilent (2.1 x 50 mm, 1.8 µm). The
165 source was equipped with a Dual AJS ESI probe operating at atmospheric pressure in
166 positive ionization mode.

167 The mobile phase was composed of ultra-pure water (MilliQ, Merck) with 0.1% (v/v)
168 formic acid (A) and acetonitrile with 0.1% (v/v) formic acid (B). The flow was set at 0.4
169 mL.min⁻¹ and the gradient program was: 0 min (5% B); 0.5 min (10% B); 4 min (10%

170 B); 9 min (10%); 13 min (25% B); 14 min (30% B); 15 min (30% B). The injection
171 volume was fixed at 1 μ L and the column temperature was maintained at 40 °C.
172 The PDA detector was set on several wavelengths: 210, 254, 285 and 320 nm. For the
173 mass detector, the parameters of the source were: gas temperature, 325 °C; gas flow, 8
174 L/min; nebulizer pressure, 35 psig; sheath gas temperature, 350 °C. The scan mode was
175 used with the following parameters: scan from 50 to 1000 m/z with a scan rate at 2;
176 capillary voltage, 3500 V; nozzle voltage, 2000 V; Fragmentor, 175 V; skimmer 1, 65
177 V; octopole, 750 V.

178

179 2.5. Analysis of growth, substrate and metabolites in fermentation broths

180 2 mL were collected at least every 2 hours during the day in each phase for 72 hours.

181 Yeast growth was measured by OD_{620 nm} using a spectrophotometer Cary 60 UV-Vis
182 from Agilent.

183 *p*-CA and 4-*vp* in aqueous and organic phase were analyzed by high-performance liquid
184 chromatography (HPLC) (Thermo scientific, Ultimate 3000) coupled with an
185 ultraviolet-diode array detector (UV-DAD) using an accucore aQ C18 column (100x3
186 mm, Thermo scientific). The injection volume was 2.5 μ L, the column temperature was
187 maintained at 48 °C and the flow rate was 0.8 mL.min⁻¹. The elution method was a 10
188 min (15 min for organic phase analysis, in this paragraph details written in brackets
189 correspond to the organic phase analysis method) gradient with acetonitrile: A and
190 formic acid 0.1%: B as mobile phases: 0 min: 5% (5%) of A – 95% (95%) of B, 3 min:
191 10% (10%) of A – 90% (90%) of B, (7.44 min: 30% of A – 70% of B), 8 min: 30%
192 (30%) of A – 70% (70%) of B and 9 min: 5% (95%) of A – 95% (5%) of B, (12 min:

193 95% of A – 5% of B, 14 min: 5% of A – 95% of B and 15 min: 5% of A – 95% of B).
194 *p*-CA was analyzed at 320 nm and its retention time was 4.3 min and 4-*vp* was analyzed
195 at 254 nm and its retention time was 8.0 min.

196 Ferulic acid was used as an internal standard. A 100 mg.L⁻¹ of ferulic acid solution in
197 acetonitrile was made and kept at -20 °C. For the aqueous samples, this solution was
198 added at 50% (v/v) to every samples before centrifugation (10000 g, 10 min).
199 Supernatants were then filtered using regenerated cellulose (RC) 0.2 µm filters. A *p*-CA
200 and a 4-*vp* calibration curves with 5 points were made using the internal standard,
201 allowing to quantify them. Organic samples were diluted at 1% (v/v) in methanol, then
202 they were mixed at 80% (v/v) with the solution of ferulic acid as internal standard and
203 finally filtered. Calibration curves with 5 points were also made in these conditions to
204 quantify *p*-CA and 4-*vp* in organic samples.

205 D-glucose and ethanol were analyzed in aqueous phases by HPLC (Thermo scientific,
206 Ultimate 3000) coupled with a Shodex refractive index detector and a Thermo scientific
207 ultraviolet detector at 210 nm and using an Aminex HPX-87H column (300x7.8 mm,
208 Bio-rad Laboratories S.A., Marnes La Coquette, France). The injection volume was 30
209 µL, the column temperature was maintained at 50 °C. Analytes were eluted isocratically
210 with 4 mM H₂SO₄ at 0.5 mL.min⁻¹ for 30 min. D-glucose and ethanol retention times
211 were 11.2 min, and 25.5 min, respectively. Samples were centrifuged at 10000 g for 5 to
212 10 min at 4 °C then mixed (50% v/v) with 4 mM H₂SO₄ and lastly, filtered using RC 0.2
213 µm filters. Calibration curves with 5 points were made in the same conditions for both
214 components to quantify them.

215

216 2.6. Respiratory *p*-CA production rate definition

217 Respiratory *p*-CA production rates ($r_{p\text{-CA}}$) were calculated by fitting *p*-CA
218 concentrations data from the first point where there is no more glucose in the broth to
219 the last point of the day (6 points) or in the case of experiments with OA addition after
220 24h: from 24 h to the first point of the next day (6 points) as a function of time, in a
221 linear model. Slopes gave us respiratory $r_{p\text{-CA}}$ with R-squared ≥ 0.8 .

222

223 2.7. *p*-CA distribution coefficient calculation

224 *p*-CA distribution coefficient between OA and fermentation broth ($\text{Log}(K_D)$) were
225 calculated as follows:

$$226 \quad \text{Log}(K_D) = \text{Log}\left(\frac{[pCA]_{OA}^{72h}}{V_{OA}^{72h}} \times \frac{V_{broth}^{72h}}{[pCA]_{broth}^{72h}}\right)$$

227 where $[pCA]_x^{72h}$ is the *p*-CA final concentration in the phase x and V_x^{72h} is the final
228 volume of phase x. Concentrations were measured according to analytical method
229 described above.

230

231 3. Results and discussion

232 3.1. A respiro-fermentative metabolism

233 A short metabolic overview of control batches at different pH or/and with different
234 media as well as cellular growth are presented in Figure 1. The major *p*-CA production
235 was observed during respiration phase, approximatively between 23 h and 48 h in every
236 experiment (Figure 1B). Such a result is in accordance with Frick and Wittmann who,
237 using flux analysis, have shown that in fermentative metabolism compared to
238 respiratory one in *S. cerevisiae*, there is a decreased carbon flux directed to the pentose

239 phosphate pathway, decreasing supply of erythrose-4-phosphate (E4P) and there is also
240 a smaller pool of phosphoenolpyruvate (PEP) available due to ethanol production (Frick
241 and Wittmann, 2005). E4P and PEP being initial substrates in the Shikimate pathway
242 leading to the formation of L-phe and L-tyr (AAA precursors of *p*-CA synthesis), this
243 decrease in carbon flux could explain *p*-CA production observed trends (Herrmann and
244 Weaver, 1999).

245 Herein, batches were conducted to study ABG010 metabolism after complete depletion
246 of carbon substrate. Indeed, as shown in Figure 1B after 48 h of cultivation for pH 6
247 experiments, a decrease in *p*-CA concentration in the broth was observed, consistent
248 with what Li et al. observed after 3 days of cultivation with their caffeic acid producing
249 *S. cerevisiae* strain (*p*-CA being the direct precursor of caffeic acid, *p*-CA was
250 accumulating in their broth as well) (Li et al., 2020). This suggests an underlying
251 consumption of *p*-CA, that could be happening from the start of experiments but
252 concealed by *p*-CA continuous biosynthesis. These results led us to investigate broth
253 compounds and identify *p*-CA degradation products accumulating in the broth. The next
254 part details and discusses these findings.

255

256 3.2. Competitive decarboxylation of *p*-coumaric acid

257 As detailed in the materials and methods section, 4-vinylphenol (4-vp, also known as *p*-
258 hydroxystyrene) - obtained through the decarboxylation of *p*-CA - was identified as the
259 main *p*-CA degradation product accumulating in the broth and its concentration was
260 measured in every samples (Figure 1E). In every batch, an accumulation of 4-vp was
261 observed in the broth suggesting that the strain of interest exhibits *p*-CA decarboxylase
262 activities. Endogenous *S. cerevisiae* phenylacrylic acid decarboxylase (PAD1) and

263 ferulic acid decarboxylase (FDC1) - whose encoding genes are not deleted in **ABG010** -
264 are suspected to be the main catalysts responsible for **decarboxylation** as it has been
265 demonstrated that they have, when both synthesized, *p*-CA decarboxylase activity
266 (Mukai et al., 2010). **Furthermore, it has been shown** that PAD1 confers a cinnamic
267 acid-resistance to the strain synthesizing it (Clausen et al., 1994). **Apart** from Li et al.
268 **(2020)** who investigated the consumption of *p*-CA in their broth and suggested the
269 involvement of PAD1 and FDC1 (Li et al., 2020), to the best of our knowledge, there is
270 no **report** of the presence of 4-*vp* in *p*-CA heterologous production using PAD1 and
271 FDC1 non-mutated *S. cerevisiae* strain. **Ro and Douglas, (2004) suggested the presence**
272 **of 4-*vp* produced by their engineered *S. cerevisiae* but could not identified it, due to the**
273 **lack of standard. For other studies, it** might be a result of the absence of 4-*vp* analytical
274 detection within these research studies due to continuous *p*-CA production.
275 One solution to avoid 4-*vp* production could be the mutation of one or the two
276 decarboxylases, but the outcome could be a high *p*-CA toxicity for the strain (Clausen et
277 al., 1994). In this case, a continuous removal of the product could address this issue, as
278 *p*-CA will not be accumulated in the medium, the toxicity issue may not be one. In the
279 case of a non-HCA decarboxylase mutated strain, a continuous extraction of the product
280 could address 4-*vp* production as *p*-CA would be less available to decarboxylation as **it**
281 **will be observed** thereafter.

282

283 **3.3. Impact of the pH and medium on the metabolism of the strain**

284 **Two pH were assessed in this work: one promoting *p*-CA extraction (i.e., pH 4.5) as it**
285 **is below *p*-CA acid moiety pKa of 4.65 (Benvidi et al., 2019; Combes et al., 2021) and**
286 **one promoting *p*-CA production (i.e., pH 6) as TAL/PAL activity requires an alkaline**

287 pH with optima around 8-9 (Jendresen et al., 2015; Sariaslani, 2007). To assess the
288 effect of pH, cultures were conducted at both pH (4.5 and 6) with YNB w/o aa medium.
289 Growths and glucose consumptions were equivalent in cultures at both pH (Figures
290 1A/1C, fermentative maximum specific growth rates (fermentative μ_{\max}) in Table 1
291 entries 5 and 9). However, in Figure 1D, a greater ethanol concentration was observed
292 in culture at pH 4.5 than at pH 6 (at maximum measured concentration, at 23 h, more
293 than twice the pH 6 ethanol concentration), demonstrating a significant difference in
294 fermentative metabolism towards ethanol production. As stated earlier, the respiration
295 phase concurring with the major part of *p*-CA production, one would expect a greater
296 production of *p*-CA at pH 4.5 due to a larger amount of ethanol accumulated, but the
297 opposite was observed (*p*-CA respiratory production rate (respiratory $r_{p\text{-CA}}$) were
298 $10.71 \pm 0.23 \text{ mg.L}^{-1} \cdot \text{h}^{-1}$ and $6.64 \pm 0.88 \text{ mg.L}^{-1} \cdot \text{h}^{-1}$ at pH 6 and 4.5, respectively). pH 6
299 may promote TAL/PAL activity as these enzymes have more alkaline optima, whereas
300 pH 4.5 may promote endogenous *S. cerevisiae* enzymes such as decarboxylases whom
301 optimum pH for this strain is 4.5-5 (Reed and Nagodawithana, 1990). As a matter of
302 fact, at pH 4.5, a significant greater final concentration of 4-vp was observed with YNB
303 w/o aa medium ($173.34 \pm 15.98 \text{ mg.L}^{-1}$ vs $87.75 \pm 11.38 \text{ mg.L}^{-1}$ for pH 6, Table 1 entries
304 5 and 9 and Figure 1E).

305 To assess the impact of the composition of the medium, an additional fermentation was
306 conducted at pH 6 using a rich and complex medium composed of yeast extract,
307 peptone and D-glucose (YEPD), and compared to the one performed with YNB w/o aa
308 at pH 6 fermentation (Figure 1 and Table 1 entries 1 and 5). More biomass was
309 produced with YEPD medium with fermentative μ_{\max} of $0.51 \pm 0.01 \text{ h}^{-1}$ and $0.38 \pm 0.03 \text{ h}^{-1}$
310 for YEPD and YNB w/o aa, respectively (Table 1 entries 1 and 5), explained by the

311 presence of metabolism precursors that allows energy saving and thus, rapid and
312 significant growth in rich media (Hahn-Hägerdal et al., 2005). In Table 1 entries 1 and
313 5, respiratory $r_{p\text{-CA}}$ are consistent with the previous observation, with 14.51 ± 0.36 and
314 $10.71 \pm 0.23 \text{ mg.L}^{-1} \cdot \text{h}^{-1}$ of $p\text{-CA}$ for YEPD and YNB w/o aa, respectively, indicating that
315 higher cell density leads to greater respiratory $r_{p\text{-CA}}$. However, at the end of the 72 h
316 fermentations, in Figure 1B there are no significant differences in $p\text{-CA}$ concentrations
317 for those two media. The fermentation end observations can be explained by the 4-vp
318 production ca. 2.6-times higher in YEPD medium ($225.86 \pm 8.44 \text{ mg.L}^{-1}$ vs 87.75 ± 11.38
319 mg.L^{-1} in YNB w/o aa medium), indicating that a significant $p\text{-CA}$ decarboxylation
320 activity may be the reason for the $p\text{-CA}$ concentration decrease in YEPD fermentations.
321 It is worth mentioning that such a decarboxylation can be favored further as YEPD
322 promotes high cell density as reported by Li et al. (2020) who investigated $p\text{-CA}$
323 consumption in rich and defined media and observed the same trends (Li et al., 2020).
324 In conclusion, compared to a defined medium such as YNB w/o aa, a rich and complex
325 medium will promote yeast growth and $p\text{-CA}$ productivity, but high $p\text{-CA}$
326 decarboxylation as well. Although continuous removal of $p\text{-CA}$ could prevent $p\text{-CA}$
327 decarboxylation with YEPD medium, YNB w/o aa was chosen to continue this study as
328 it will ease recovery process while being consistent with previous preliminary
329 experiments (Combes et al., 2021).

330

331 3.4. Extractive biphasic fermentations

332 Figure 2 shows $p\text{-CA}$ (A) and 4-vp (B) total production concentrations as functions of
333 time for biphasic experiments using OA as extractant and corresponding controls
334 experiments with YNB w/o aa as culture medium. Table 1 complements those data with

335 details and key parameters of those experiments (entries 2, 3, 4, 6, 7 and 8).

336 Significant differences between control experiments using nutsparger and dissolved
337 oxygen regulation, and control experiments using sintered-microsparger observed in
338 Table 1 entries 4, 5, 8 and 9 (mainly on fermentative μ_{\max} parameter) could be explained
339 by excess dissolved oxygen levels when using sintered-microsparger (dissolved oxygen
340 did not decrease below 70% of saturation in those experiments). The use of those
341 spargers for biphasic experiments and corresponding controls is described in details in
342 the materials and methods section. Consequently, in this part, biphasic experiments will
343 be compared to control experiments conducted with sintered-microsparger.

344 In the first 24 hours, *p*-CA total productions seemed equivalent for a given pH (Figure
345 2A). However, after around 30 hours, one can observe that the addition of OA from the
346 outset resulted in a greater *p*-CA total production in biphasic system for both pH, the
347 highest *p*-CA total productions being achieved at pH 6 (Figure 2A). A significant
348 increase of the respiratory r_{p-CA} is observed when *p*-CA was removed from the start
349 (Table 1, entries 2 and 4, pH 6: $13.65 \pm 0.21 \text{ mg.L}^{-1}.\text{h}^{-1}$ of *p*-CA vs $11.07 \pm 1.08 \text{ mg.L}^{-1}.\text{h}^{-1}$
350 for the corresponding control; entries 6 and 8, pH 4.5: $9.45 \pm 0.04 \text{ mg.L}^{-1}.\text{h}^{-1}$ of *p*-CA vs
351 $7.18 \pm 0.06 \text{ mg.L}^{-1}.\text{h}^{-1}$ for the corresponding control). These results are even more
352 interesting if one looks at the density of biomass producing *p*-CA. Indeed, fermentative
353 μ_{\max} for biphasic fermentation with OA addition at 0 h were equivalent to those of
354 corresponding control experiments, meaning that the same number of cells produced a
355 greater amount of *p*-CA through respiration in biphasic fermentations with OA addition
356 at 0 h compared to controls (Table 1, entries 2, 4, 6 and 8). Therefore, there might be a
357 significant impact of OA phase presence from the beginning on ABG010 respiratory r_{p-CA} .
358 CA.

359

360 3.5. Study of the time of addition of oleyl alcohol

361 As exponential and rapid growth occurs during glucose consumption and the main *p*-
362 CA production occurs after this phase, addition of extractive OA phase after total
363 glucose consumption, at 24 h was thus investigated. The aim was to avoid any negative
364 effect of OA on growth, to start *p*-CA recovery with a high driving force and with the
365 hypothesis that it will further increase respiratory $r_{p\text{-CA}}$. In experiments where OA was
366 added after 24 h of cultivation, 6 h from OA addition, on the contrary, trends suggested
367 lower *p*-CA production than control ones in both pH assessed (Figure 2A). For example,
368 at pH 6, respiratory $r_{p\text{-CA}}$ for the biphasic experiment was $6.97 \pm 1.76 \text{ mg.L}^{-1}.\text{h}^{-1}$ vs
369 $11.07 \pm 1.08 \text{ mg.L}^{-1}.\text{h}^{-1}$ for the control (Table 1 entries 3 and 4). To conclude, even
370 though growths were control equivalents, respiratory $r_{p\text{-CA}}$ decreased widely when the
371 OA phase was added after complete glucose consumption. Although this outcome was
372 not further investigated, nor any report found about this behavior in the literature, a
373 certain adaptive mechanism of ABG010 must be involved, and enabled when grown
374 with OA from the start. Another explanation could also be a change in metabolism due
375 to OA presence, equivalent to an external stress response when added after 24 h. For the
376 next step, results and discussion will be focused on experiments with direct addition of
377 OA and corresponding controls.

378

379 3.6. Impact of biphasic fermentation on *p*-CA decarboxylation

380 At the end of the experiment carried out at pH 4.5 with OA added at 0 h (ca. 72 h), *p*-
381 CA final total production was found significantly greater than the corresponding control

382 one (Figure 2A, Table 1 entries 6 and 8). A reduced decarboxylation activity could
383 explain partly this observation, as in the case of continuous extraction of *p*-CA at pH 4.5
384 the final total production of 4-*vp* was less than half that of the control one (57.97 ± 10.67
385 $\text{mg}\cdot\text{L}^{-1}$ and $123.76\pm 12.64 \text{ mg}\cdot\text{L}^{-1}$, respectively) (Figure 2B and Table 1 entries 6 and 8).
386 Indeed, at pH 4.5, *p*-CA was mostly distributed in the organic phase (Figure 3 and Table
387 1 entries 6 and 8) with a final distribution coefficient between OA and the broth
388 ($\text{Log}(K_D)$) of 0.98 ± 0.15 and less than $50 \text{ mg}\cdot\text{L}^{-1}$ of *p*-CA in the aqueous phase at all
389 times, reducing drastically the extent of decarboxylation by ABG010 enzymes. For
390 biphasic experiment at pH 6, final total *p*-CA production was equivalent to the
391 corresponding control (Figure 2A). While 4-*vp* final total production was significantly
392 lower than the control (Table 1 entries 2 and 4), the difference was not as wide as for
393 pH 4.5. As a result, both biphasic experiments with addition of OA at the beginning had
394 equivalent 4-*vp* total production (Table 1 entries 2 and 6). As shown in Figure 3, at pH
395 6, *p*-CA was mostly distributed in the aqueous phase, i.e., the broth, with a $\text{Log}(K_D)$ of -
396 0.23 ± 0.02 (Table 1 entry 2), which could account for the lower 4-*vp* final total
397 production difference with the control in comparison with observations at pH 4.5. It is
398 also noteworthy to mention that, in biphasic experiments, 4-*vp* was mostly distributed in
399 the organic phase, with less than $5 \text{ mg}\cdot\text{L}^{-1}$ in the broth at all times (Data not shown).
400 Indeed, 4-*vp* is a hydrophobic solute, with a $\text{Log}(P_{o/w})$ of 2.4 (Computed by XLogP3
401 3.0). This result could impair final purity in the organic phase, and thus, suggests that if
402 a high purity is needed, a decrease or abolition of *S. cerevisiae p*-CA decarboxylation
403 activities (by deletion of genes encoding relevant enzymes) or an additional downstream
404 process step could be required.

405

406 3.7. Extractive biphasic fermentation, an adaptable process

407 To summarize, with ABG010 strain, the highest respiratory $r_{p\text{-CA}}$ reached in this study
408 was in biphasic fermentation with addition of OA at the beginning and pH 6 for the
409 broth ($13.65 \pm 0.21 \text{ mg} \cdot \text{L}^{-1} \cdot \text{h}^{-1}$ of $p\text{-CA}$) (Table 1 entry 2). This result undoubtedly
410 demonstrates the high potential of a LLE-ISPR for the heterologous $p\text{-CA}$ production
411 using an engineered *S. cerevisiae*. Nevertheless, one can expect a different outcome
412 with a strain producing greater amount of $p\text{-CA}$ where toxicity and solubility might be
413 an issue. The hypothesis is that, in this study, these latter factors are not limiting, and
414 thus, the increase in respiratory $r_{p\text{-CA}}$ in biphasic system was not as significant as it has
415 been for other biosynthesized inhibiting solute, like in the work of Kim et al. (2020)
416 who successfully increased caproic acid microbial productivity by 5.8-fold using OA
417 and Alamine 336 as extractant. With a more advanced engineered strain, with a higher
418 $p\text{-CA}$ production rate, or with glucose-limited fed-batch implementation in addition to
419 the proposed LLE-ISPR process, productivity could be even higher.

420 As far as pH is concerned, pH 4.5 brings significant benefits since it allows $p\text{-CA}$ to be
421 mostly distributed in the organic phase allowing a detoxification and a high percentage
422 of recovery whereas, at pH 6, the highest $r_{p\text{-CA}}$ was obtained but an acidification of the
423 broth may be needed at the end of the fermentation to recover $p\text{-CA}$.

424 The medium is another parameter that could also be investigated further, as YNB w/o aa
425 would be economically challenging for an industrial production. Therefore, the
426 implementation of a complex medium implementation or the definition of minimal
427 optimized medium could be explored. Although a complex medium could be
428 disadvantageous for phase separation and final purity, it would allow significant growth

429 whereas a defined and minimal medium would ease product recovery but could be
430 limiting for strain growth.

431

432 4. Conclusion

433 In this work for the first time, a LLE-ISPR process for the intensification of *p*-CA
434 heterologous production was implemented, using an engineered *S. cerevisiae* strain and
435 oleyl alcohol as extractant, showing the promising potential of this approach. Optimal
436 respiratory *p*-CA production rates were obtained in biphasic experiments with OA
437 addition at 0 h of cultivation at pH 4.5 and 6. With ABG010, the highest *p*-CA
438 respiratory production rate was obtained at pH 6, in biphasic fermentation. Furthermore,
439 it was confirmed that the continuous extraction of *p*-CA significantly prevented its
440 decarboxylation in the broth.

441

442 **E-supplementary data**

443 Mass spectrum of 4-vinylphenol in sample can be found in e-version of this paper
444 online.

445

446 **Competing interests**

447 The authors declare that they have no competing interests.

448

449 **Availability of data and materials**

450 The datasets used and/or analyzed during the current study are available from the
451 corresponding author on reasonable request.

452

453 **Funding**

454 This work was supported by the Agence Nationale de la Recherche (ANR, Grant ANR-
455 17-CE07-0046), Région Grand Est (France), Conseil Départemental de la Marne
456 (France), and Grand Reims (France).

457

458 **Authors' contributions**

459 FA conceived and acquired the financial support for the whole concept of the ANR-17-
460 CE07-0046 project leading to this publication. J Combes, NI and ML conceived the
461 study and designed the experiments. CF engineered and provided the strain. J Combes,
462 NI, J Couvreur, and BG performed the fermentations. FB performed analysis on LC-
463 MS. J Combes analyzed and interpreted data. J Combes wrote the manuscript. NI, FA
464 and ML reviewed the manuscript. All authors read and approved the final manuscript.

465

466 **Acknowledgements**

467 The authors thank Dr. Louis Mouterde for the synthesis of 4-vinylphenol.

468

469 **References**

- 470 1. Aversch, N.J.H., Kayser, O. (Eds.), 2020. Biotechnological Production and
471 Conversion of Aromatic Compounds and Natural Products. Frontiers Research
472 Topic. Frontiers Media SA. <https://doi.org/10.3389/978-2-88963-913-7>
- 473 2. Baranowski, J.D., Davidson, P.M., Nagel, C.W., Branen, A.L., 1980. Inhibition
474 of *Saccharomyces cerevisiae* by naturally occurring hydroxycinnamates. J. Food
475 Sci. 45, 592–594. <https://doi.org/10.1111/j.1365-2621.1980.tb04107.x>

- 476 3. Benvidi, A., Dadras, A., Abbasi, S., Tezerjani, M.D., Rezaeinasab, M., Tabaraki,
477 R., Namazian, M., 2019. Experimental and computational study of the pK_a of
478 coumaric acid derivatives. *J. Chin. Chem. Soc.* 66, 589–593.
479 <https://doi.org/10.1002/jccs.201800265>
- 480 4. Boo, Y.C., 2019. *p*-Coumaric Acid as An Active Ingredient in Cosmetics: A
481 Review Focusing on its Antimelanogenic Effects. *Antioxidants* 8, 275.
482 <https://doi.org/10.3390/antiox8080275>
- 483 5. Clausen, M., Lamb, C.J., Megnet, R., Doerner, P.W., 1994. PAD1 encodes
484 phenylacrylic acid decarboxylase which confers resistance to cinnamic acid in
485 *Saccharomyces cerevisiae*. *Gene* 142, 107–112. [https://doi.org/10.1016/0378-](https://doi.org/10.1016/0378-1119(94)90363-8)
486 [1119\(94\)90363-8](https://doi.org/10.1016/0378-1119(94)90363-8)
- 487 6. Combes, J., Clavijo Rivera, E., Clément, T., Fojcik, C., Athès, V., Moussa, M.,
488 Allais, F., 2021. Solvent selection strategy for an ISPR (*In Situ*/In stream
489 product recovery) process: The case of microbial production of *p*-coumaric acid
490 coupled with a liquid-liquid extraction. *Sep. Purif. Technol.* 259, 118170.
491 <https://doi.org/10.1016/j.seppur.2020.118170>
- 492 7. Cuellar, M.C., Straathof, A.J.J., 2018. Chapter 4: Improving Fermentation by
493 Product Removal, in: *Intensification of Biobased Processes*. pp. 86–108.
494 <https://doi.org/10.1039/9781788010320-00086>
- 495 8. Dafoe, J.T., Daugulis, A.J., 2014. *In situ* product removal in fermentation
496 systems: improved process performance and rational extractant selection.
497 *Biotechnol. Lett.* 36, 443–460. <https://doi.org/10.1007/s10529-013-1380-6>

- 498 9. Davidson, P.M., Taylor, T.M., Schmidt, S.E., 2013. Chemical Preservatives and
499 Natural Antimicrobial Compounds, in: *Food Microbiology: Fundamentals and*
500 *Frontiers*, M. P., Doyle; R., Buchanan. American Society for Microbiology.
501 765–801. <https://doi.org/10.1128/9781555818463.ch30>
- 502 10. Flourat, A.L., Combes, J., Bailly-Maitre-Grand, C., Magnien, K., Haudrechy,
503 A., Renault, J., Allais, F., 2020. Accessing *p*-Hydroxycinnamic Acids:
504 Chemical Synthesis, Biomass Recovery, or Engineered Microbial Production?
505 *ChemSusChem* 14, 118-129. <https://doi.org/10.1002/cssc.202002141>
- 506 11. Freeman, A., Woodley, J.M., Lilly, M.D., 1993. *In Situ* Product Removal as a
507 Tool for Bioprocessing. *Nat Biotechnol* 11, 1007–1012.
508 <https://doi.org/10.1038/nbt0993-1007>
- 509 12. Frick, O., Wittmann, C., 2005. Characterization of the metabolic shift between
510 oxidative and fermentative growth in *Saccharomyces cerevisiae* by comparative
511 ¹³C flux analysis. *Microb. Cell Factories* 4, 30. [https://doi.org/10.1186/1475-](https://doi.org/10.1186/1475-2859-4-30)
512 [2859-4-30](https://doi.org/10.1186/1475-2859-4-30)
- 513 13. Gold, N.D., Gowen, C.M., Lussier, F.-X., Cautha, S.C., Mahadevan, R., Martin,
514 V.J.J., 2015. Metabolic engineering of a tyrosine-overproducing yeast platform
515 using targeted metabolomics. *Microb. Cell Factories*, 14:73, 1-16.
516 <https://doi.org/10.1186/s12934-015-0252-2>
- 517 14. Hahn-Hägerdal, B., Karhumaa, K., Larsson, C.U., Gorwa-Grauslund, M.,
518 Görgens, J., van Zyl, W.H., 2005. Role of cultivation media in the development

- 519 of yeast strains for large scale industrial use. *Microb. Cell Factories* 4, 31.
520 <https://doi.org/10.1186/1475-2859-4-31>
- 521 15. Hartmann, M., Schneider, T.R., Pfeil, A., Heinrich, G., Lipscomb, W.N., Braus,
522 G.H., 2003. Evolution of feedback-inhibited / barrel isoenzymes by gene
523 duplication and a single mutation. *Proc. Natl. Acad. Sci.* 100, 862–867.
524 <https://doi.org/10.1073/pnas.0337566100>
- 525 16. Hazelwood, L.A., Daran, J.-M., van Maris, A.J.A., Pronk, J.T., Dickinson, J.R.,
526 2008. The Ehrlich Pathway for Fusel Alcohol Production: a Century of Research
527 on *Saccharomyces cerevisiae* Metabolism. *Appl. Environ. Microbiol.* 74, 2259–
528 2266. <https://doi.org/10.1128/AEM.02625-07>
- 529 17. Heeres, A.S., Picone, C.S.F., van der Wielen, L.A.M., Cunha, R.L., Cuellar,
530 M.C., 2014. Microbial advanced biofuels production: overcoming emulsification
531 challenges for large-scale operation. *Trends Biotechnol.* 32, 221–229.
532 <https://doi.org/10.1016/j.tibtech.2014.02.002>
- 533 18. Herrmann, K.M., Weaver, L.M., 1999. The shikimate pathway. *Annu Rev Plant*
534 *Physiol Plant Mol Biol* 32. <https://doi.org/10.1146/annurev.arplant.50.1.473>
- 535 19. Higuchi, T., 1981. Biosynthesis of Lignin, in: Tanner, W., Loewus, F.A. (Eds.),
536 *Plant Carbohydrates II: Extracellular Carbohydrates*, Encyclopedia of Plant
537 *Physiology*. Springer, Berlin, Heidelberg, pp. 194–224.
538 https://doi.org/10.1007/978-3-642-68234-6_9

- 539 20. Huccetogullari, D., Luo, Z.W., Lee, S.Y., 2019. Metabolic engineering of
540 microorganisms for production of aromatic compounds. *Microb. Cell Factories*
541 18, 41. <https://doi.org/10.1186/s12934-019-1090-4>
- 542 21. Humphreys, J.M., Chapple, C., 2002. Rewriting the lignin roadmap. *Curr. Opin.*
543 *Plant Biol.* 5, 224–229. [https://doi.org/10.1016/S1369-5266\(02\)00257-1](https://doi.org/10.1016/S1369-5266(02)00257-1)
- 544 22. Hyun, M.W., Yun, Y.H., Kim, J.Y., Kim, S.H., 2011. Fungal and Plant
545 Phenylalanine Ammonia-lyase. *Mycobiology* 39, 257–265.
546 <https://doi.org/10.5941/MYCO.2011.39.4.257>
- 547 23. Jendresen, C.B., Stahlhut, S.G., Li, M., Gaspar, P., Siedler, S., Förster, J.,
548 Maury, J., Borodina, I., Nielsen, A.T., 2015. Highly Active and Specific
549 Tyrosine Ammonia-Lyases from Diverse Origins Enable Enhanced Production
550 of Aromatic Compounds in Bacteria and *Saccharomyces cerevisiae*. *Appl.*
551 *Environ. Microbiol.* 81, 4458–4476. <https://doi.org/10.1128/AEM.00405-15>
- 552 24. Kim, H., Choi, O., Jeon, B.S., Choe, W.-S., Sang, B.-I., 2020. Impact of
553 feedstocks and downstream processing technologies on the economics of caproic
554 acid production in fermentation by *Megasphaera elsdenii* T81. *Bioresource*
555 *Technology* 301, 122794. <https://doi.org/10.1016/j.biortech.2020.122794>
- 556 25. Koopman, F., Beekwilder, J., Crimi, B., van Houwelingen, A., Hall, R.D.,
557 Bosch, D., van Maris, A.J., Pronk, J.T., Daran, J.-M., 2012. *De novo* production
558 of the flavonoid naringenin in engineered *Saccharomyces cerevisiae*. *Microb.*
559 *Cell Factories* 11, 155. <https://doi.org/10.1186/1475-2859-11-155>

- 560 26. Li, Y., Mao, J., Liu, Q., Song, X., Wu, Y., Cai, M., Xu, H., Qiao, M., 2020. *De*
561 *Novo* Biosynthesis of Caffeic Acid from Glucose by Engineered *Saccharomyces*
562 *cerevisiae*. ACS Synth. Biol. 9, 756–765.
563 <https://doi.org/10.1021/acssynbio.9b00431>
- 564 27. Liu, J., Du, C., Beaman, H.T., Monroe, M.B.B., 2020. Characterization of
565 Phenolic Acid Antimicrobial and Antioxidant Structure–Property Relationships.
566 Pharmaceutics 12, 419. <https://doi.org/10.3390/pharmaceutics12050419>
- 567 28. Liu, Q., Liu, Y., Chen, Y., Nielsen, J., 2020. Current state of aromatics
568 production using yeast: achievements and challenges. Curr. Opin. Biotechnol.
569 65, 65–74. <https://doi.org/10.1016/j.copbio.2020.01.008>
- 570 29. Liu, Q., Yu, T., Li, X., Chen, Yu, Campbell, K., Nielsen, J., Chen, Yun, 2019.
571 Rewiring carbon metabolism in yeast for high level production of aromatic
572 chemicals. Nat. Commun. 10, 4976. [https://doi.org/10.1038/s41467-019-12961-](https://doi.org/10.1038/s41467-019-12961-5)
573 5
- 574 30. Luttik, M.A.H., Vuralhan, Z., Suir, E., Braus, G.H., Pronk, J.T., Daran, J.M.,
575 2008. Alleviation of feedback inhibition in *Saccharomyces cerevisiae* aromatic
576 amino acid biosynthesis: Quantification of metabolic impact. Metab. Eng. 10,
577 141–153. <https://doi.org/10.1016/j.ymben.2008.02.002>
- 578 31. Mortimer, R.K., Johnston, J.R., 1986. Genealogy of Principal Strains of the
579 Yeast Genetic Stock Center. Genetics 113, 35–43.

- 580 32. Mouterde, L.M.M., Allais, F., 2018. Microwave-Assisted Knoevenagel-Doebner
581 Reaction: An Efficient Method for Naturally Occurring Phenolic Acids
582 Synthesis. *Front. Chem.* 6. <https://doi.org/10.3389/fchem.2018.00426>
- 583 33. Mukai, N., Masaki, K., Fujii, T., Kawamukai, M., Iefuji, H., 2010. PAD1 and
584 FDC1 are essential for the decarboxylation of phenylacrylic acids in
585 *Saccharomyces cerevisiae*. *J. Biosci. Bioeng.* 109, 564–569.
586 <https://doi.org/10.1016/j.jbiosc.2009.11.011>
- 587 34. Nijkamp, K., Westerhof, R.G.M., Ballerstedt, H., de Bont, J.A.M., Wery, J.,
588 2007. Optimization of the solvent-tolerant *Pseudomonas putida* S12 as host for
589 the production of *p*-coumarate from glucose. *Appl. Microbiol. Biotechnol.* 74,
590 617–624. <https://doi.org/10.1007/s00253-006-0703-0>
- 591 35. Pei, K., Ou, J., Huang, J., Ou, S., 2016. *p*-Coumaric acid and its conjugates:
592 dietary sources, pharmacokinetic properties and biological activities: *p*-
593 Coumaric acid and its conjugates. *J. Sci. Food Agric.* 96, 2952–2962.
594 <https://doi.org/10.1002/jsfa.7578>
- 595 36. Reed, G., Nagodawithana, T.W., 1990. *Yeast Technology*. Springer
596 Netherlands, Dordrecht. <https://doi.org/10.1007/978-94-011-9771-7>
- 597 37. Ro, D.-K., Douglas, C.J., 2004. Reconstitution of the Entry Point of Plant
598 Phenylpropanoid Metabolism in Yeast (*Saccharomyces cerevisiae*): Implications
599 for control of metabolic flux into the phenylpropanoid pathway. *J. Biol. Chem.*
600 279, 2600–2607. <https://doi.org/10.1074/jbc.M309951200>

- 601 38. Rodriguez, A., Kildegaard, K.R., Li, M., Borodina, I., Nielsen, J., 2015.
602 Establishment of a yeast platform strain for production of *p*-coumaric acid
603 through metabolic engineering of aromatic amino acid biosynthesis. *Metab. Eng.*
604 31, 181–188. <https://doi.org/10.1016/j.ymben.2015.08.003>
- 605 39. Santos, A.G., Albuquerque, T.L. de, Ribeiro, B.D., Coelho, M.A.Z., 2020. *In*
606 *situ* product recovery techniques aiming to obtain biotechnological products: A
607 glance to current knowledge. *Biotechnol. Appl. Biochem.* n/a.
608 <https://doi.org/10.1002/bab.2024>
- 609 40. Sariaslani, F.S., 2007. Development of a Combined Biological and Chemical
610 Process for Production of Industrial Aromatics from Renewable Resources.
611 *Annu. Rev. Microbiol.* 61, 51–69.
612 <https://doi.org/10.1146/annurev.micro.61.080706.093248>
- 613 41. Stark, D., Stockar, U. von, 2003. *In Situ* Product Removal (ISPR) in Whole Cell
614 Biotechnology During the Last Twenty Years. *Process Integr. Biochem. Eng.*
615 149–175. https://doi.org/10.1007/3-540-36782-9_5
- 616 42. Van Hecke, W., Kaur, G., De Wever, H., 2014. Advances in *in-situ* product
617 recovery (ISPR) in whole cell biotechnology during the last decade. *Biotechnol.*
618 *Adv.* 32, 1245–1255. <https://doi.org/10.1016/j.biotechadv.2014.07.003>
- 619 43. Varga, A., Bata, Z., Csuka, P., Bordea, D.M., Vértessy, B.G., Marcovici, A.,
620 Irimie, F.D., Poppe, L., Bencze, L.C., 2017. A novel phenylalanine ammonia-
621 lyase from *Kangiella koreensis*. *Stud. Univ. Babeş-Bolyai Chem.* 62, 293–308.
622 <https://doi.org/10.24193/subbchem.2017.3.25>

623 44. Yang, S.-T., Lu, C., 2013. Extraction-Fermentation Hybrid (Extractive
624 Fermentation), in: Ramaswamy, S., Huang, H.-J., Ramarao, B.V. (Eds.),
625 Separation and Purification Technologies in Biorefineries. John Wiley & Sons,
626 Ltd, Chichester, UK, pp. 409–437. <https://doi.org/10.1002/9781118493441.ch15>

627

628 Table 1: Details, key parameters and data on study experiments

629 Figure 1: ABG010 control batches assessing YEPD and YNB without amino acids (w/o
630 aa) media and pH 4.5 and 6 results as a function of time. A: ABG010 growth, $\ln(X/X_0)$;
631 B: *p*-CA concentration in the broth in mg.L^{-1} ; C: glucose concentration in the broth in
632 g.L^{-1} ; D: ethanol concentration in the broth in g.L^{-1} ; E: 4-vinylphenol concentration in
633 the broth in mg.L^{-1} . All data represent the mean of $n = 2$ independent samples and error
634 bars show standard deviation

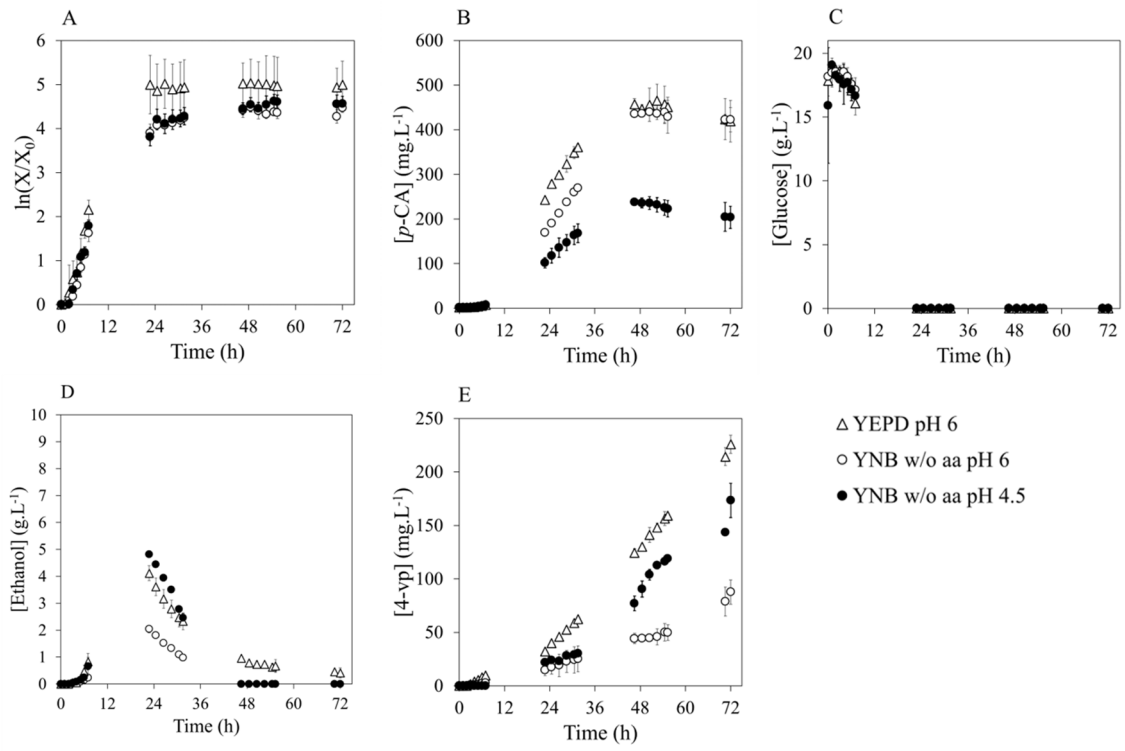
635 Figure 2: Total production concentrations (obtained from mass balance calculation in
636 each phase for biphasic experiments and expressed per volume of broth) of A: *p*-
637 coumaric acid and B: 4-vinylphenol as a function of time for the assessment of pH and
638 OA addition time effect on biphasic batch fermentation with YNB w/o aa medium. All
639 data represent the mean of $n = 2$ independent samples and error bars show standard
640 deviation except for “pH 4.5 – OA addition after 24 h” where $n = 1$.

641 Figure 3: *p*-CA distribution in biphasic experiments using OA as organic phase since 0
642 h of cultivation.

643

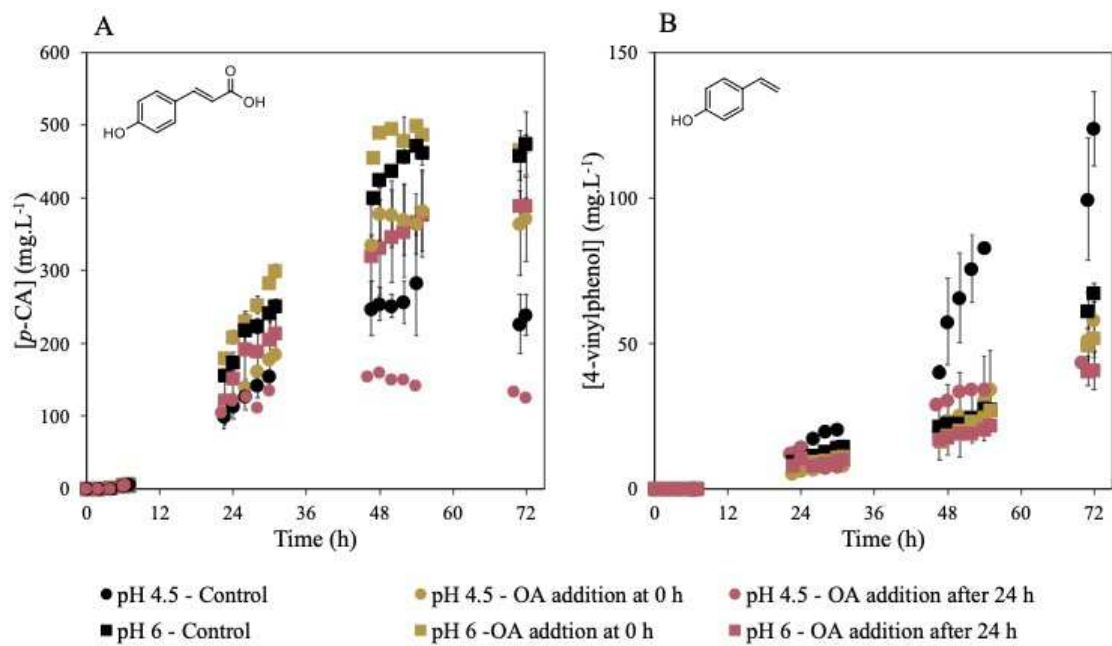
Entry	Medium	pH	OA addition time (h) ^a	Type of sparger ^b	Mixing rate (rpm)	Fermentative μ_{\max} (h ⁻¹)	Respiratory r_{p-CA} (mg.L ⁻¹ .h ⁻¹)	4-vp final production mg.L ⁻¹	$p-CA$ Log (K _D) at 72 h ^a
1	YEPD	6	N/A	NS	350-900	0.51±0.01	12.91±0.55	225.86±8.44	N/A
2	YNB	6	0	Sintered	75	0.23±0.00	13.65±0.21	51.79±6.59	- 0.23±0.02
3	YNB	6	24	Sintered	75	0.26±0.03	6.97±1.76	40.64±10.98	- 0.23±0.08
4	YNB	6	N/A	Sintered	75	0.29±0.06	11.07±1.08	67.23±3.20	N/A
5	YNB	6	N/A	NS	350-900	0.38±0.03	10.50±0.51	87.75±11.38	N/A
6	YNB	4.5	0	Sintered	75	0.18±0.01	9.45±0.04	57.97±10.67	0.98±0.15
7	YNB	4.5	24	Sintered	75	0.18 ^c	1.44 ^c	51.84 ^c	1.00 ^c
8	YNB	4.5	N/A	Sintered	75	0.20±0.02	7.18±0.06	123.76±12.64	N/A
9	YNB	4.5	N/A	NS	350-900	0.34±0.01	7.53±0.85	173.34±15.98	N/A

644 ^a N/A stands for Not Applicable, meaning experiments are not biphasic; ^b NS stands for
645 nutsparger; ^c Experiment with no duplicate; In bold: first experiments discussed, control
646 batches with nutsparger and regulation of dissolved oxygen.



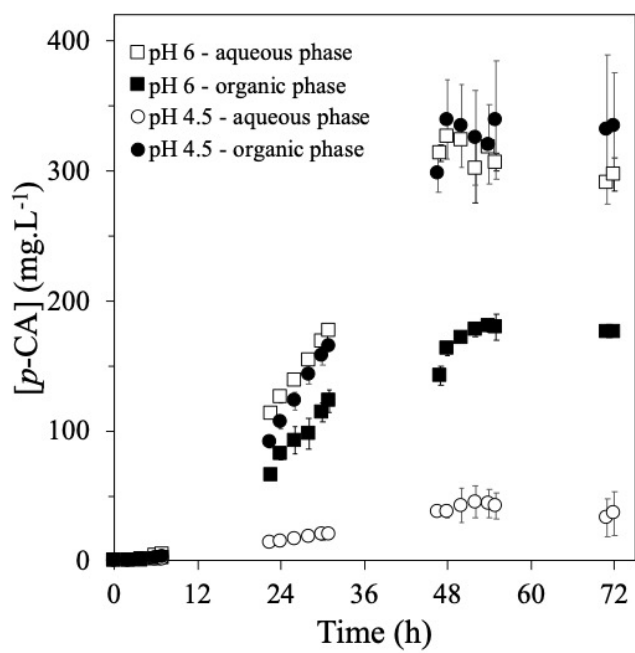
647

648



649

650



651